Penerbit Akademia Baru

CFD Letters

Journal homepage: www.akademiabaru.com/cfdl.html
ISSN: 2180-1363

The Effect of Vortex Generators on Aerodynamics for Sedan Cars

Open Access

Bassem Nashaat Zakher[1*], Mostafa El-Hadary[2], Andrew Nabil Aziz[3]

[1] Faculty of Engineering, Pharos University in Alexandria (PUA), Egypt
[2] Faculty of Engineering, Alexandria University, Egypt
[3] City of Scientific Research and Technological Application (SRTA-city), Egypt

ARTICLE INFO

Article history:
Received 5 March 2019
Received in revised form 9 May 2019
Accepted 9 June 2019
Available online 2 July 2019

Keywords:
CFD; drag coefficient; simulation; aerodynamics (Aero)

ABSTRACT

Energy saving and protecting the global environment are the main issues of this time, with fuel consumption crises becoming the most concerned topic in automotive development. The aerodynamic (Aero) drag for sedan vehicles is a result of the separation of flow near the vehicle's rear end. To minimise the separation, a bump-shaped vortex generator (VG) is used at the back end of a sedan. The main aim of this work is to study the effect of VGs on the drag coefficient (DC) for modern sedan cars at different velocities. CFD code FLUENT was used to evaluate the flow distribution around the Fabia Sedan. The results were used to evaluate the DC by calculating the drag force acting on the body. In addition, the results indicate that CFD flow simulation is a useful tool for providing predictions of pressure distribution and forces exerted on the vehicle components.

1. Introduction

The aerodynamics (Aero) of vehicles has been studied since the 1920's and 1930's [1,2]. However, it was only in recent times that the tools for studying it have become so powerful, especially when using powerful simulation tools such as COMSOL and Ansys which are employed in different fields [3-5]. After looking at the forces that play the greatest role in determining a car's efficiency, it was said that the shape of the car and its aerodynamics are the most important in design. The aim of the manufacturer is to build a car to reach the limits of the Aero in a way that can be mass-produced. In planning an Aero car, researchers and designers paid attention to the shape of the front end, its underbody, its air ducts to the radiator, its compartment ventilation, its loading, and all exterior obstacles. Thus, the Aero must have balance with the safety, stability and comfort of the passenger. Road vehicles are now the subject of extensive research on Aero forces in terms of both lift and drag. Modern cars have an average DC of about 0.35, based upon the frontal area since the frontal area has also decreased sharply. The minimum DC reached 0.15 for a tear-shaped vehicle, which could be achieved any time the public is willing to purchase such a shape [6]. The external flow over a road

* *Corresponding author.*
E-mail address: Bassem.zakher@pua.edu.eg (Bassem Nashaat Zakher)

vehicle is usually determined by complex three-dimensional vortex wake interactions and regions of massive separation. The accurate prediction of the dynamics of this behaviour still constitutes a challenge to numerical simulations, especially to turbulence modelling approaches.

John and Kristian [7] presented a wake analysis and measurements behind road vehicles. The wake is caused by severe separation from many different regions and the vehicle geometry acts as a bluff body. The separation gives low pressure in the base region, the back of the vehicle, and often strong longitudinal vortices accompanied by a large magnitude cross flow that extracts kinetic energy from the flow. Since the total drag is traditionally split up into pressure drag and vortex drag, the right techniques are needed to measure both to be able to distinguish or separate them and their relative importance and contribution to the total drag. In order to improve the car in terms of CD via geometrical changes, it is important to know the structure of the wake. For example, a large cross flow giving rise to regions of large vorticity or swirling vertical flow is a dictation of a large vortex drag. Measurements of these cross-flow velocities are not simple measurements but essential in order to trace the longitudinal vortices emanating from separation. By measuring the wake flow field, either clockwise or counter clockwise, the vortex can be found on each side of the plane of symmetry, with the direction depending on the slant angle. The reduction in drag would then be coupled with the elimination of the vortex drag produced by the upper rear part of the body.

Koike *et al.,* [8] presented a study on the reduction of Aero drag by VGs. Adding dimple-shaped pieces can lower the DC to a fraction of its original value due to a change in the critical Reynolds (Re) number, where the transition from laminar to turbulent flow begins in the boundary layer. The main aim of using VGs is to control flow separation at the end of a sedan car when the critical Re number is exceeded. VGs increase both the delaying of the flow separation and the drag force by itself. To find the optimum VG geometry, the thickness of the boundary layer is measured according to the assumption that the optimum height of the VG would be nearly equal to the boundary layer thickness. As for the shape, a bump-shaped piece with a rear slope angle of 25° to 30° was selected (according to the experimental results from Ahmed's model). As for the location of VGs, a point directly upstream of the flow separation point was supposed to be the optimum and a point of 100 mm in front of the roof end was selected.

Gillieron and Chometon [9] developed a numerical simulation using (k-ε) model of the fluent software and compared the results of the DC with the experimental results obtained by Ahmed *et al.,* [10]. They also described the wake flow behaviour for angles ranging between zero and lower critical angle and between lower and upper critical angles. They also considered values above the upper critical angle. Their results showed that the numerical simulation was a highly promising method for investigating the physical phenomenon in automotive Aero. From the obtained results on the shapes of Ahmed's reference model, it would appear possible to include computational methods in the analytical phases of a vehicle's development cycle. This is because the friction for Ahmed's reference model is identical to those observed on an actual vehicle.

Siti Ruhliah and Mohamed Sukri [11] compared the Detached-Eddy Simulation (DES) of high Re flow and the noise between Large Eddy Simulation (LES) around rod-airfoil. The study indicated that both the simulations provided the current study with a recognisable vortex core, which is apposite enough for the study of leading-edge noise examination. Nevertheless, the LES model is believed to have a more defined grid resolution that can provide a better performance.

Krajnovic and Davidson [12] estimated the computational grid needed for the representation of the near wall structures in a Large Eddy Simulation (LES) of the flow around cars. They showed that approximately $6x10^8$ cells are needed in the near wall region of a simplified car-like shape. However, they found the similarity of the flows at different Re numbers. From this, they established that LES of the flow around a car at lower Re numbers can be useful for a qualitative understanding of the flow

around a car at high Re numbers. This study aimed not only to investigate the feasibility of LES in Aero vehicles but also to indicate the usefulness of LES for the understanding of the flow around vehicles. Both the instantaneous and the time-averaged flows are described using their LES results.

Spohn and Gillieron [13] stated that the Aero forces on road vehicles were the result of complex interactions between the dynamic behaviour of the released vortex wake and flow separations. Efficacious future car designs need to take the benefit of these interactions to improve flow control by means of active or passive control devices. Detailed knowledge of the physical mechanisms involved in the formation of flow separations and their interactions with vortex wakes is necessary to achieve this objective since the experiments were conducted in a closed water tunnel. The test-bed had a rectangular cross-section of 0.5 x 0.25 m^2 and a length of 1.4 m. The upper limitation of the test section was left open with a free surface. In addition, the flow speed varied between 0.10 m/sec and 0.30 m/sec with $3x10^4$ = Re = $9x10^4$, where the Re number is based on the length of the Ahmed model's body. All sidewalls were made of clear Perspex to allow flow visualisation. A lateral water evacuation by cyclones was permitted to observe the flow through the end wall of the test-section in the upstream direction. The flow was visualised with the help of the electrolytic precipitation technique.

Kanagaraj and Periyasamy [14] presented a research in the influence of VG in Aero device, which consisted of a small vane attached for lifting the surface, for instance a rotor blade of a wind turbine or an aircraft wing. VGs may also be involved in some parts of an Aero vehicle such as fuselage of an aircraft or a car. When the body is in motion relative to the air, the VG creates a vortex, which, by removing some parts of the slow-moving boundary layer in contact with the airfoil surface, delays local flow separation and Aero stalling, which thus improves the effectiveness of wings and control surfaces, for instance flaps and rudders.

Sivaraj *et al.,* [15] described that the VG is an Aero surface which consists of a small vane or bump that generates a vortex. VGs delay Aero stalling and flow separation, thus improving control surfaces and the effectiveness of wings. We have chosen VG as our Aero device to be implemented in the sedan car to enhance the performance of the car. VGs were developed for the aircraft area, and this knowledge has made its way into car design. The main purpose of this device is to delay air flow separation. Air flow separation is when the airflow of an object detaches from the surface and creates eddies and vortexes. Thus, VG over the rear of the roof effectively helps to reduce drag.

2. Methodology

2.1 Numerical Details

2.1.1 Governing equations

The governing equations of fluid flow characterize mathematical statements of the conservation laws of physics:

i. Fluid's mass is conservation
ii. The change of momentum's rate equals the sum of the forces for a fluid particle.
iii. The rate of change of energy is equal to the sum of the rate of heat addition and the rate of work done on a fluid particle.

2.1.2 Mass conservation in three dimensions

For the fluid element, the rate of increase of its mass is equal to the net rate of flow of mass into the controlled volume. This yields:

$$\frac{\partial \rho}{\partial t}+\frac{\partial(\rho u)}{\partial x}+\frac{\partial(\rho v)}{\partial y}+\frac{\partial(\rho w)}{\partial z}=0$$

Or written in vector notation as:

$$\frac{\partial \rho}{\partial t}+div(\rho \mathbf{u})=0 \tag{1}$$

For incompressible fluid in the fluid element, the rate of increase of its mass is equal to the rate of flow of mass into the controlled volume.

Eq. (1) is the unsteady, three-dimensional mass conservation or continuity equation at a point in a compressible fluid. For an incompressible fluid, the density, ρ is constant and Eq. (1) becomes

$$div\mathbf{u}=0 \tag{2}$$

Or in a longhand notation:

$$\frac{\partial u}{\partial x}+\frac{\partial v}{\partial y}+\frac{\partial w}{\partial z}=0 \tag{3}$$

2.1.3 Momentum equation in three dimensions

Newton's second law states that the rate of change of momentum of a fluid particle equals the sum of the forces on the particle. The rates of increase of x-, y- and z- momentum per unit volume of a fluid particle are given by:

$$\rho\frac{Du}{Dt} \qquad \rho\frac{Dv}{Dt} \qquad \rho\frac{Dw}{Dt} \tag{4}$$

There are two types of forces on fluid particles:

i. Surface forces: pressure forces and viscous forces.
ii. Body forces: gravity force, centrifugal force, Coriolis force and electromagnetic force.
iii. The body forces' overall effect is defined by the sources S_{Mx}, S_{My} and S_{Mz} of the x-component, y-component and z-component of the momentum equation.

Thence, the momentum of the x-component equation is given by:

$$\rho\frac{Du}{Dt}=\frac{\partial(-p+\tau_{xx})}{\partial x}+\frac{\partial \tau_{yx}}{\partial y}+\frac{\partial \tau_{zx}}{\partial z}+S_{Mx} \tag{5}$$

For y-component of the momentum, the equation is given by:

$$\rho \frac{Dv}{Dt} = \frac{\partial \tau_{xy}}{\partial x} + \frac{\partial(-p + \tau_{yy})}{\partial y} + + \frac{\partial \tau_{zy}}{\partial z} + S_{My} \tag{6}$$

The momentum equation for z is determined by:

$$\rho \frac{Du}{Dt} = \frac{\partial \tau_{xz}}{\partial x} + \frac{\partial \tau_{yz}}{\partial y} + \frac{\partial(-p + \tau_{zz})}{\partial z} + S_{Mz} \tag{7}$$

2.1.4 Navier–Stokes equations for a Newtonian fluid

The governing equations contain further unknowns for the viscous stress components. The most useful forms of the conservation equations for fluid flows are obtained by introducing a suitable model for the viscous stress, τ_{ij}. In many fluid flows, the viscous stresses can be stated as functions of the local deformation rate (strain rate). In 3D flows, the local rate of the deformation is collected in the linear deformation rate and the volumetric deformation rate. The three linear elongating deformation components are determined by:

$$e_{xx} = \frac{\partial u}{\partial x} \qquad e_{yy} = \frac{\partial v}{\partial y} \qquad e_{zz} = \frac{\partial w}{\partial z} \tag{8}$$

There are also six shearing linear deformation components:

$$e_{xy} = e_{yx} = \frac{1}{2}\left(\frac{\partial u}{\partial y} + \frac{\partial v}{\partial x}\right) \qquad e_{xz} = e_{zx} = \frac{1}{2}\left(\frac{\partial u}{\partial z} + \frac{\partial w}{\partial x}\right) \qquad e_{yz} = e_{zy} = \frac{1}{2}\left(\frac{\partial v}{\partial z} + \frac{\partial w}{\partial y}\right) \tag{9}$$

The volumetric deformation is given by:

$$\frac{\partial u}{\partial x} + \frac{\partial v}{\partial y} + \frac{\partial w}{\partial z} = div\mathbf{u} \tag{10}$$

Substitution of these stresses into the momentum equations (Eq. (5), Eq. (6) and Eq. (7)) yields the so-called Navier–Stokes equations named after the two 19th century scientists who derived them independently. Thence, the x-component of the NS equation is given by:

$$\rho \frac{Du}{Dt} = -\frac{\partial p}{\partial x} + div(\mu grad u) + S_{Mx} \tag{11}$$

The y-component of the NS equation is given by:

$$\rho \frac{Dv}{Dt} = -\frac{\partial p}{\partial y} + div(\mu grad v) + S_{My} \tag{12}$$

The z-component of the NS equation is given by:

$$\rho \frac{Dw}{Dt} = -\frac{\partial p}{\partial z} + div(\mu grad w) + S_{Mz} \tag{13}$$

2.1.5 Transport equation models

There are significant commonalties between the various equations (Eq. (11), Eq. (12) and Eq. (13)). If a general variable, ϕ is introduced on the conservative form of all fluid flow equations, the following equation will be developed:

$$\frac{\partial(\rho\phi)}{\partial t} + div(\rho\phi \mathbf{U}) = div(\Gamma grad\phi) + S_\phi \tag{14}$$

Integrating Eq. (14) over a 3D control volume CV yields:

$$\frac{\partial}{\partial t}\left(\int_{CV} \rho\phi dV\right) + \int_A \mathbf{n}.(\rho\phi\mathbf{U})dA = \int_A \mathbf{n}.(\Gamma grad\phi)dA + \int_{CV} S_\phi dV \tag{15}$$

2.2 Solver Details

Hybrid cars are a new technology in the automobile industry; however, they do not have the power capabilities of a normal car. Thus, it is essential to minimise the external Aero drag by optimising the shape of the car. The efficiency of an Aero CFD simulation depends, therefore, on the time span essential to achieve the first set of results, in addition to the accuracy of the simulated flow quantities [9]. The turns around time and confidence level in the predictions are two major criteria for success that complete one another. Creation of the model geometry, discretisation of the physical domain, and choice of an appropriate numerical calculating scheme are significant factors that can determine the level of success of such an effort.

2.3 Geometry Description for The Sedan Car Body

The sedan car body (e.g. Fabia sedan model) is 4.222 m long, 1.449 m high and 1.424 m wide, with a projected area of 1.449 m^2 for the 2D results width of 1 m, as shown in Figure 1.

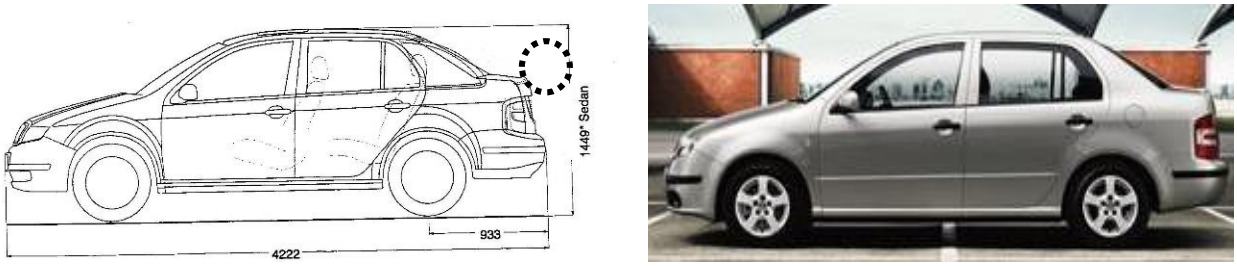

Fig. 1. The geometry description for 2D sedan car model

Because of the presence of a trunk at the rear of the body, the flow separates at the roof end and then separates downwards. So, adding dimple-shaped pieces can lower the DC to a fraction of its original value because dimples cause a change in the turbulence characteristics, even though the

purpose of using VGs is to control flow separation at the roof ends of the body. Figure 2 shows the geometry and location of VG on the sedan body.

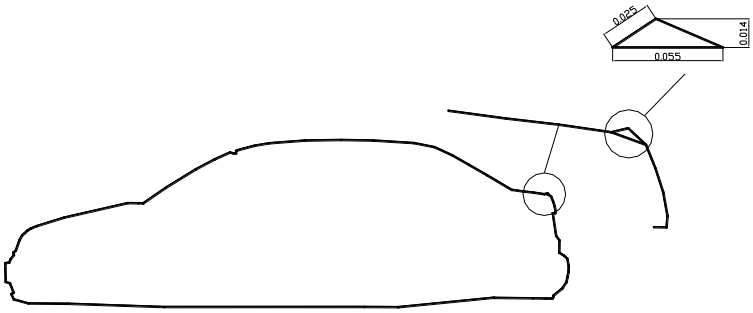

Fig. 2. Location of VGs at the sedan body

2.4 Domain and Mesh Grid Description for The Sedan Car Body

In the 2D model, the stream-wise direction of the body section was kept in the mid plane of the car and the flow domain was chosen similar to the one taking place in the Ahmed model's body [10]. The Aero forces applied on the body are the product of compound interactions between the dynamic behavior of the released vortex wake and flow separations. The principle contribution to drag experienced by the car is the pressure drag. The rear of the vehicle provides a major contribution to this pressure drag. Thus, the rear design is crucial in defining the mode of the wake flow and therefore, the drag experienced by the vehicle. The mesh grid for the domain around the sedan car is revealed in Figure 3.

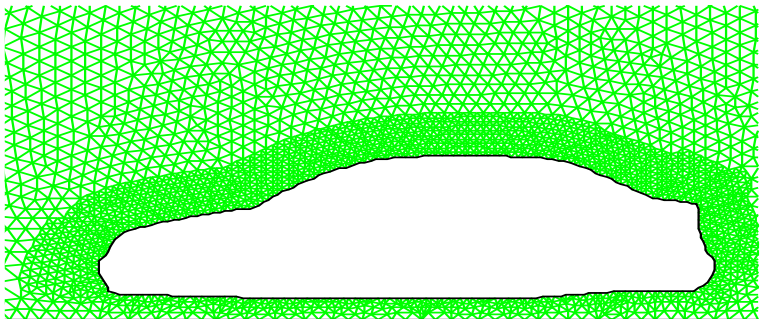

Fig. 3. The mesh grid of the sedan car body

Because the flow in question is turbulent near the wall, treatment is of increased importance. The turbulent models in software FLUENT [16] cannot be taken all the way to the wall of the boundary. Thus, the first node must be chosen above the laminar and buffer layer and in the logarithmic layer. A non-dimensional vertical coordinate y+ was used to find the location of the first node for the wall function approach. For the wall function method, the first grid point must be chosen so that y+ is between 50 to 500. The DC, C_D was calculated for a car length, L=4.222 m and a projected area =1.449 m^2**.**

For different car velocities, the C_D is calculated from:

$$C_D = \frac{F}{0.5\rho u^2 A} = \frac{F}{0.8875u^2} \tag{12}$$

Where, F is the total drag resulting from pressure and viscous effects.

The Re number is calculated from:

$$Re = 2.89 \times u \times 10^5 \quad (12)$$

2.5 Model Validation

This validation was achieved by applying all parameters used in Koike and his team's study [8]. The model output showed good agreement qualitatively with Masaru's model. The solution of the set of equations given in the previous section was done using Ansys, which is a software based on the finite volume method by changing the model geometry from Masaru's model to this sedan car. After a grid independent analysis, the complete mesh consisting of 20797 triangular cells was taken for the geometry chosen (see Figure 3). Mesh independent test methodology for Roache [17] was used. The numerical model started to converge at N1=20797 elements. The computations were made for the following cases:

i. Original body design.
ii. The car body without the VGs.
iii. The car body with the proposed 25 mm vortex generator.

3. Results

Figure 4 shows the effect of Re number on DC for the sedan body of the original design. As the Re number was increased from 48.167x10^5 to 80.178x10^5, the DC decreased from 0.3271 to 0.3229. Increasing the Re number over approximately 80.278x10^5 resulted in an increase in the DC to 0.389 at Re number equals to 115.6x10^5.

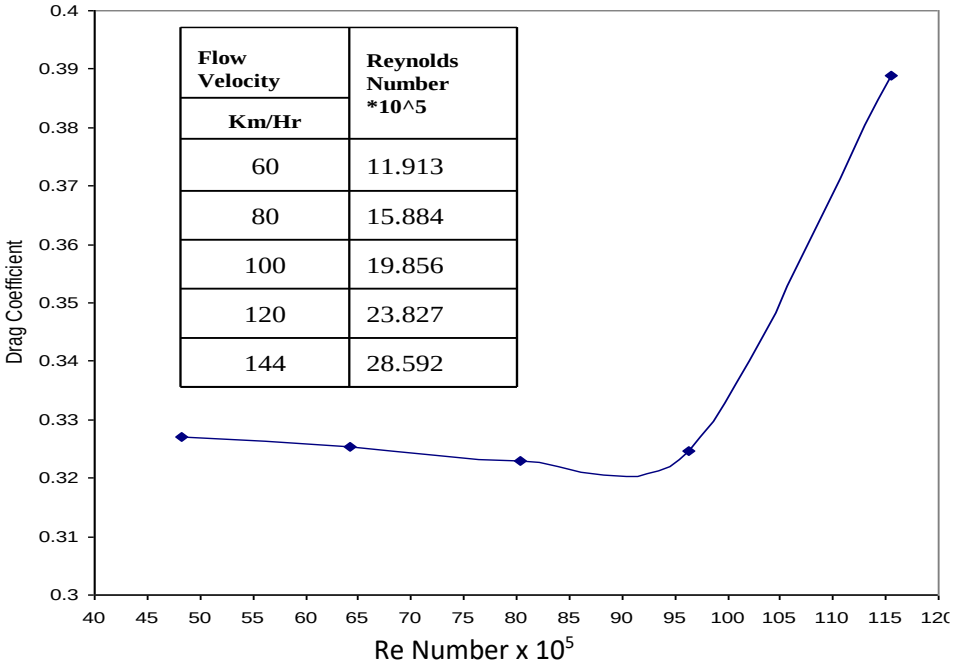

Fig. 4. Effect of Re number on DC for the sedan car body of original body design

From Figures 5 (a), (b), (c), (d) and (e), it is seen that when the Re number is below 80.178x10^5, no appreciable change in the system of vortices takes place in the wake of the body. But for larger values of Re Number, although the system of vortices is more or less the same in shape, the kinetic energy associated with them increased in strength considerably.

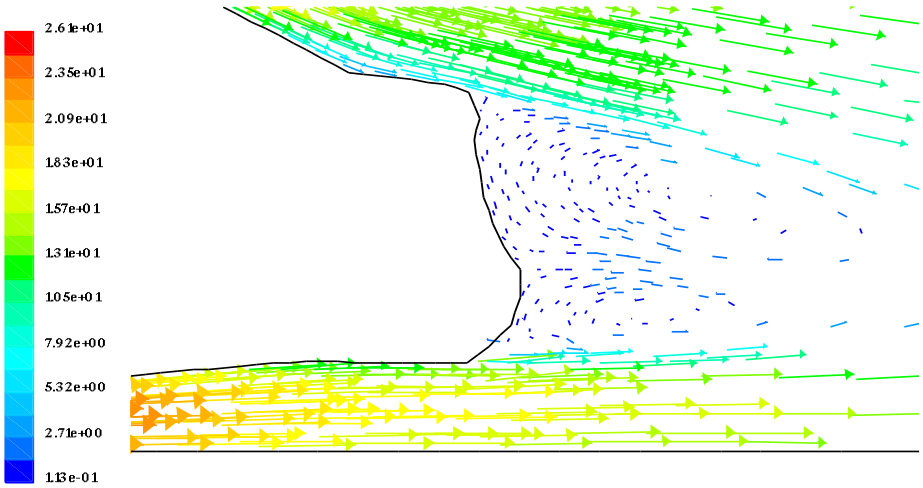

(a) For (Re=48.167x10^5, C_D=0.3271

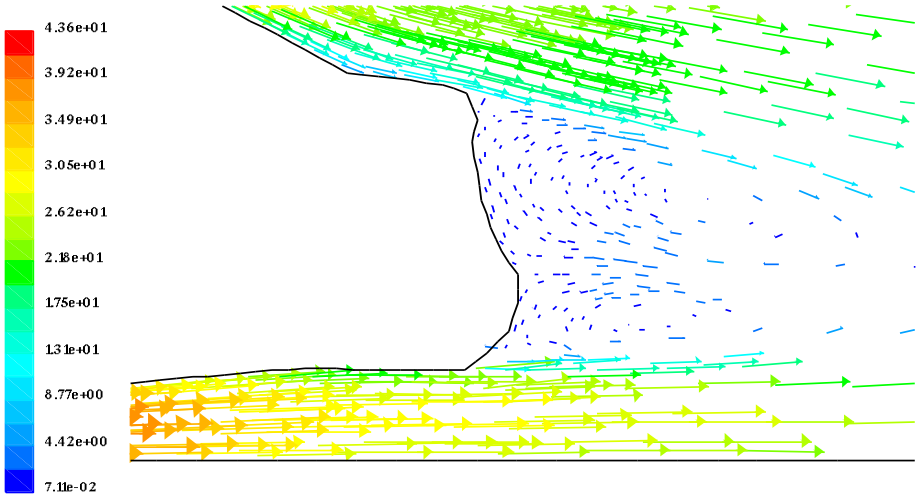

(b) For (Re=64.222x10^5, C_D=0.3254

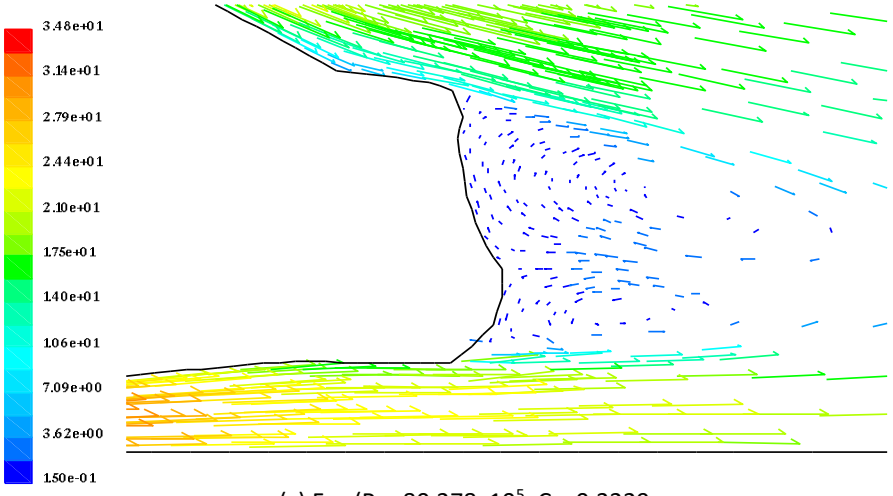

(c) For (Re=80.278x10^5, C_D=0.3229

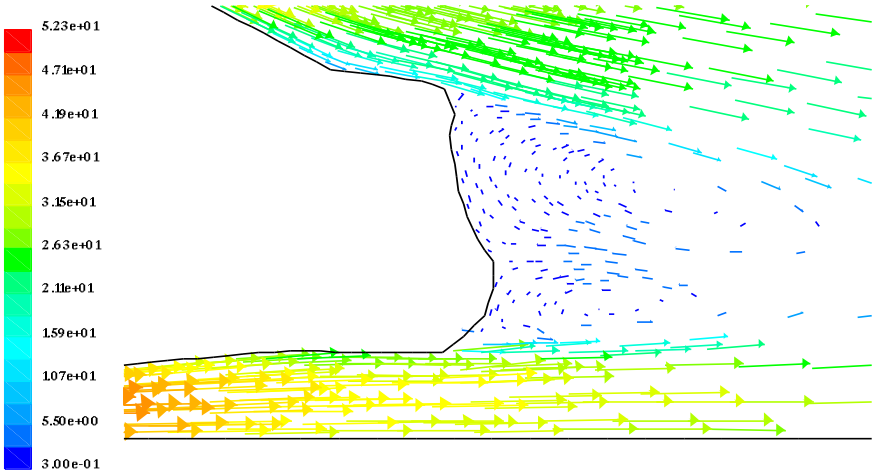

(d) For (Re=96.333x10^5, C_D=0.324

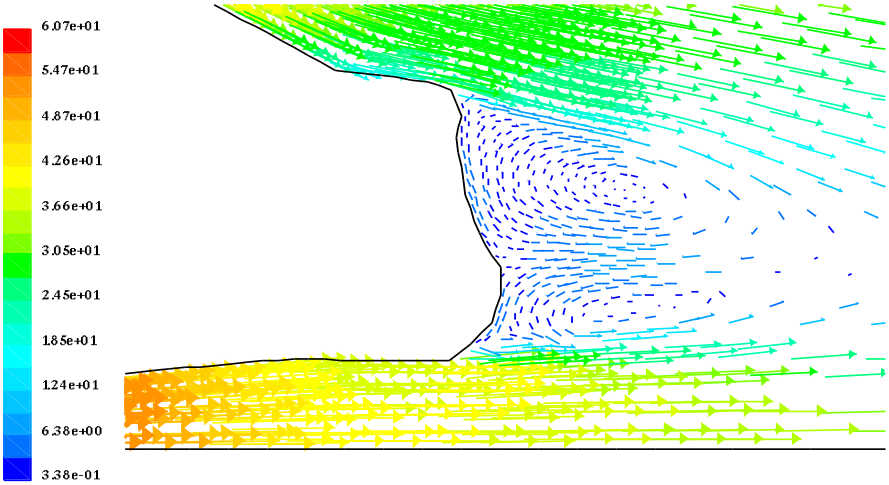

(e) For (Re=115.6x10^5, C_D=0.389

Fig. 5. Velocity vectors for the sedan car body in the original design

Figure 6 shows the effect of Re number on DC for the modified sedan car body without a vortex generator. This modification led to a complete change in the relationship between the DC and Re number for the same range of the latter compared to the original design. For Re number below approximately 80.278x10^5, the DC increased as the Re number is increased. The opposite holds true for Re > 80.278x10^5.

Figures 7 (a), (b), (c), (d) and (e) show the velocity vectors for the sedan car body without a vortex generator. It is seen from the figures that although the system of vortices at different Re numbers is more or less the same in nature, it is clear that the opposing vortex generated in the wake zone is weaker at Re =80.278x10^5 than those at smaller and larger values of Re This enables the main vortex to attain higher kinetic energy, thus producing a region of lower pressure on the back side of the car and effectively increasing the DC.

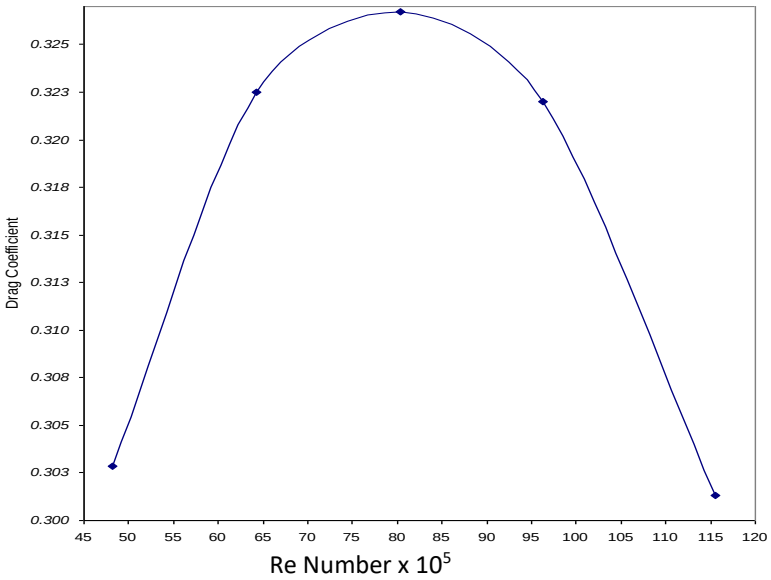

Fig. 6. Effect of Re number on DC for the sedan car body without a vortex generator

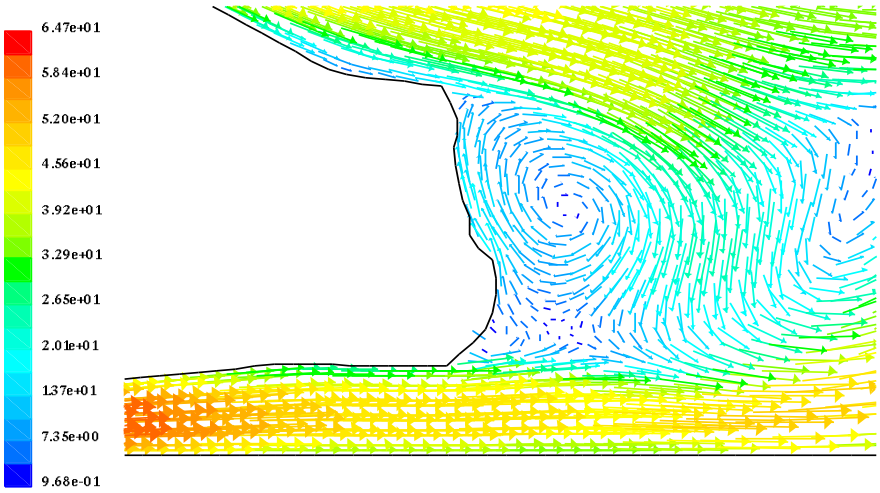

(a) For Re=48.167x10^5, C_D=0.3028

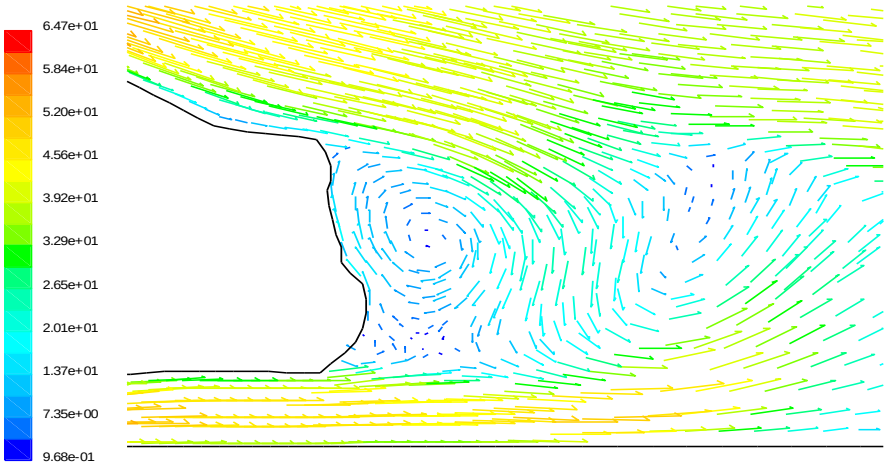

(b) For Re=64.222x10^5, C_D=0.3225

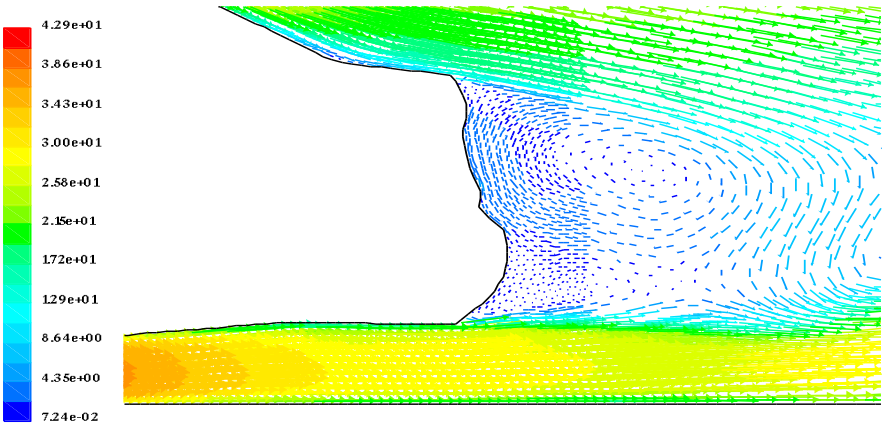

(c) For Re=80.278x10^5, C_D=0.3267

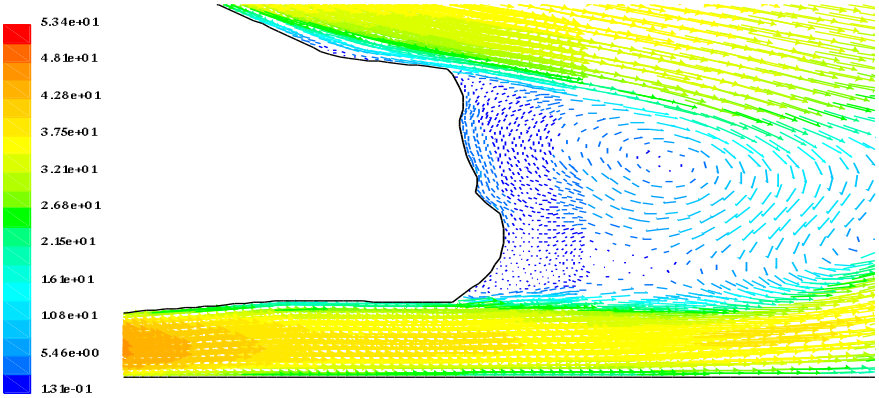

(d) For Re=96.333x10^5, C_D=0.322

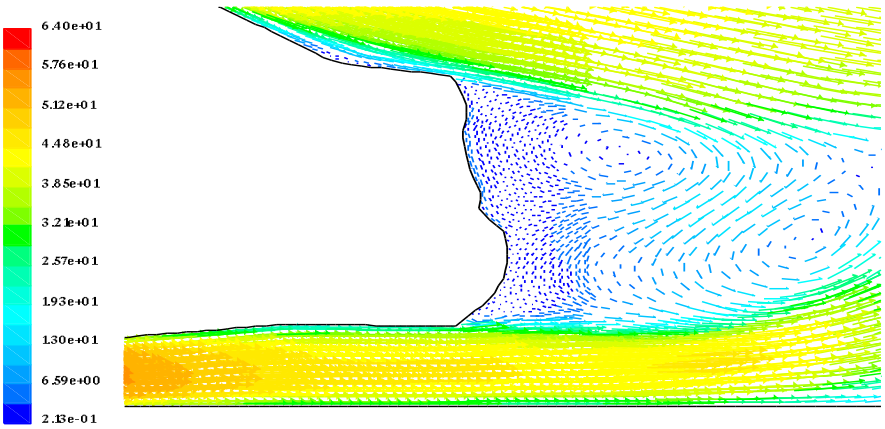

(e) For Re=115.6x10^5, C_D=0.3013

Fig. 7. Velocity vectors for the sedan car body without a vortex generator (VG)

Figure 8 shows the effect of Re number on DC for the sedan body with 25 mm height of delta wing-shaped vortex generator. This modification led to a decrease in the DC to 0.235 at Re=96.333 x 10^5. As the Re number increased from 48.167 x 10^5 to 64.222 x 10^5, a small change in DC took place (from 0.3439 to 0.3444). However, when the Re number increased to about 96.333 x10^5, the DC decreased to reach a lower value of 0.235, and when increasing the Re number (Re>96.33x10^5), the DC increased sharply.

Figures 9 (a), (b), (c), (d), (e) and (f) show the velocity vectors for the sedan body with 25 mm VG at different Re numbers. From the figures, it is seen that the opposed vortex is stronger at Re=96.333 x 10^5 (approximately) compared to smaller or larger values of Re This results in a smaller amount of

kinetic energy attained by the main vortex, causing a relative increase in the pressure in the wake and thereby a decrease in the DC.

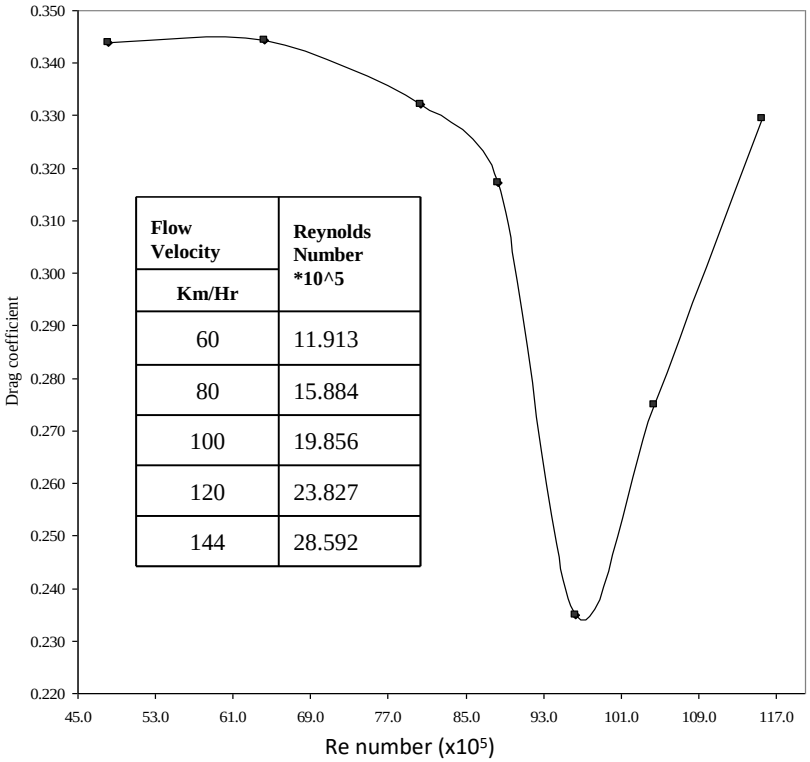

Flow Velocity Km/Hr	Reynolds Number *10^5
60	11.913
80	15.884
100	19.856
120	23.827
144	28.592

Fig. 8. Effect of Re number on drag coefficient (DC) for the sedan car body with a 25 mm vortex generator (VG)

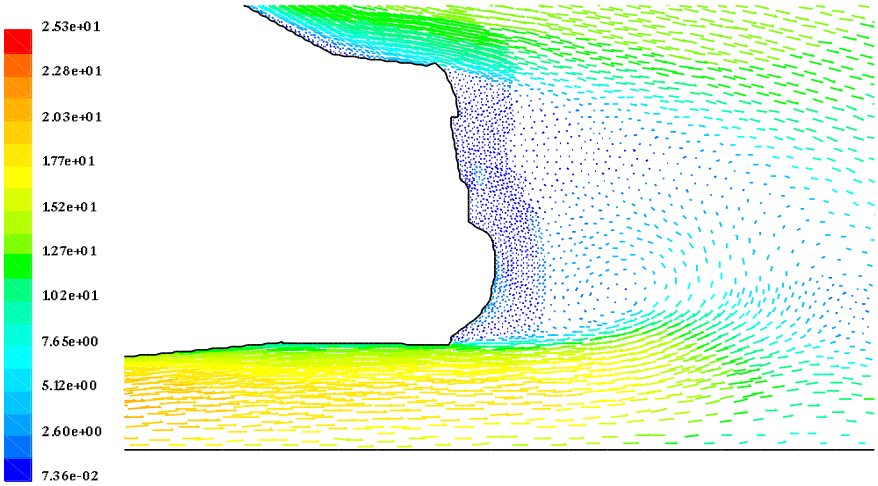

(a) For Re=48.167x10^5, C_D=0.3439

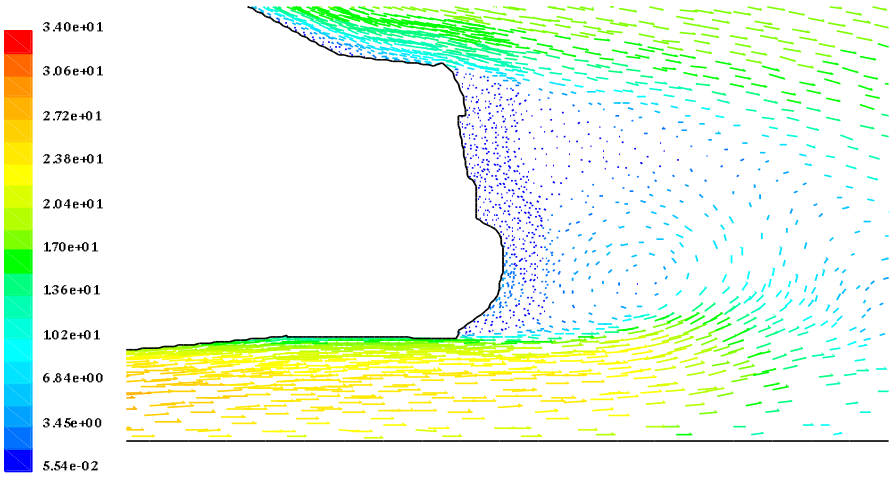

(b) For Re=64.222x10^5, C_D=0.3444

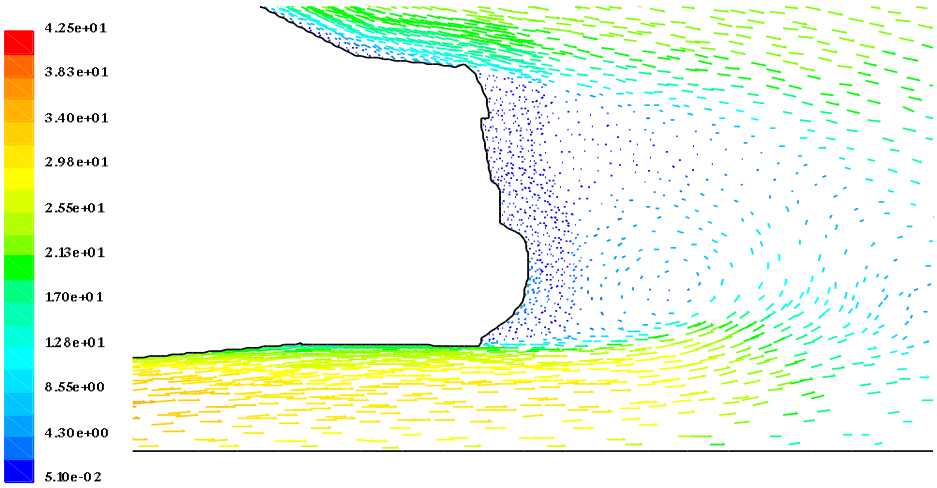

(c) For Re=80.278x10^5, C_D=0.322

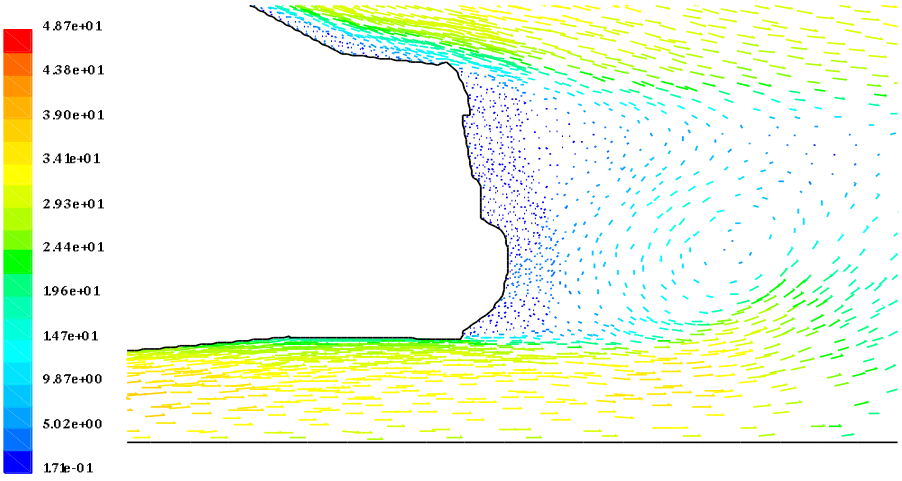

(d) For Re=88.303x10^5, C_D=0.3171

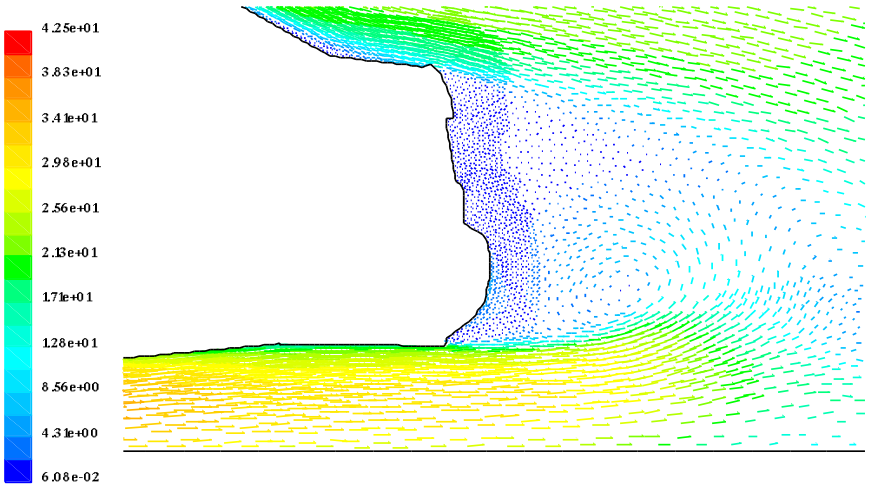

(e) For (Re=96.333 x10^5, CD=0.235

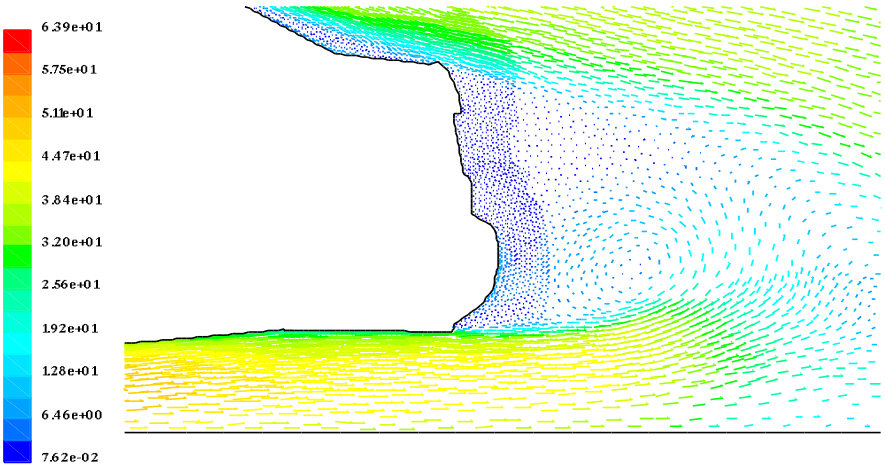

(f) For Re=115.6x10^5, C_D=0.3294

Fig. 9. Velocity vectors for the sedan car body with a 25 mm vortex generator (VG)

Figure 10 is a reproduction of Figure 4, Figure 6 and Figure 8, showing the effect of the Re number on DC for the sedan car body for different rear designs. For lower values of Re number, the results for various designs agreed qualitatively and the differences in the DC reached a value of 10% for the smallest value of Re number considered. For Re values larger than 85x10^5 up to approximately 96 x 10^5, the differences in DC between the original design and without VG were well below 3%. On the other hand, when a 25 mm VG was used, the differences in DC reached approximately 40%. For values of Re larger than about 96x10^5, the results of the 25 mm VG and the original design agreed well qualitatively and showed a marked increase in the DC. In this range of Re number, the percentage change in DC for the case without VG was of order 10%. It is clear from the results that there is nothing that can be considered as the optimum design for the car rear for the whole range of Re in terms of the whole car speed range. VGs are recommended for relatively higher speeds, while the original design is recommended for lower car speeds.

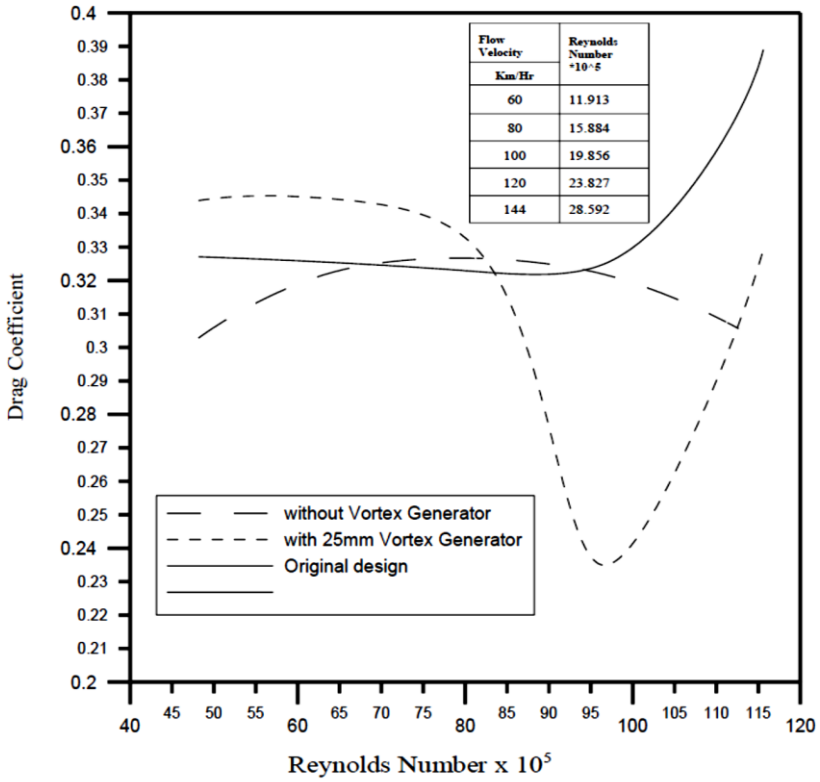

Fig. 10. Effect of Re number on drag coefficient (DC) for a sedan car

4. Conclusions

In this paper, a two-dimensional model for a sedan car was developed using the Ansys fluent software and was compared to existing results in the literature. VGs installed at the sedan's rear end are found to improve the Aero characteristics with a height of 25 mm. VGs having a height of 25 mm are found to improve the Aero characteristic of the car rear in general. It is concluded here that there is nothing that can be considered as the optimum design for the car rear shape to cover the whole range of car speed. VGs are recommended to be installed for higher car speeds, while the original design is preferred for lower car speeds.

References

[1] Munson, Bruce R., Donald F. Young, and Theodore H. Okiishi. "Fundamentals of Fluid Mechanics, John Wiley & Sons." *Inc., USA* (2006).

[2] Manaf, Muhammad Zaki Abdul, Shabudin Mat, Shuhaimi Mansor, Mohd Nazri Nasir, Tholudin Mat Lazim, Wan Khairuddin Wan Ali, Wan Zaidi Wan Omar et al.,. "Influences of External Store on Aerodynamic Performance of UTM-LST Generic Light Aircraft Model." *Journal of Advanced Research in Fluid Mechanics and Thermal Sciences* 39, no. 1 (2017): 36-46.

[3] Abdullah, Amira Lateef, Suhaimi Misha, Noreffendy Tamaldin, and Mohd Afzanizam Mohd. "Numerical Analysis of Solar Hybrid Photovoltaic Thermal Air Collector Simulation by ANSYS." *CFD Letters* 11, no. 2 (2019): 1-11.

[4] Andrew N. Aziz, M. Elsayed Youssef, Mohammed A. Hassab, and Wael M. El-Maghlany. "Performance Analysis of DMFC and PEMFC Numerically with Models Validation." *International Journal of Advances in Electronics and Computer Science* 5, no. 4 (2018): 14-17.

[5] Aziz, Andrew N., Omar O. Rabhy, and M. Elsayed Youssef. "Modeling and Experimental investigation for PEMFC to achieve high Fuel Cell performance." In *Int. Conf. New Trends Sustain. Energy-ICNTSE, Pharos University and KTH VETENSKAP OCH KONST*, pp. 228-31. 2016.

[6] B. N. Zakher, M. A. El-Gohary, I.M. El fahham, and H.A. El-Gamal. "Computational Fluid Dynamics Results for Ahmed's car model." *International Journal of Advanced Scientific and Technical Research* 6, no.6 (2016): 194-210.

[7] John G-S. and Kristian A., "Wake analysis and measurements.", SAE Technical papers series 840302., 2000.
[8] Koike, Masaru, Tsunehisa Nagayoshi, and Naoki Hamamoto. "Research on aerodynamic drag reduction by vortex generators." *Mitsubishi motors technical review* 16 (2004): 11-16.
[9] Chometon, F., and P. Gillieron. "A survey of improved techniques for analysis of three-dimensional separated flows in automotive aerodynamics." In *SAE Congress, Detroit, Michigan*, pp. 27-29. 1996.
[10] Ahmed, S. R. "Influence of base slant on the wake structure and drag of road vehicles." *Journal of fluids engineering* 105, no. 4 (1983): 429-434.
[11] S.R. Lizarose Samion , Mohamed Sukri Mat Ali. "Comparison of Rod-Airfoil Noise Calculation between Large Eddy Simulation (LES) and Detached-Eddy Simulation (DES)" *CFD Letters* 11, no.2 (2019): 12-20.
[12] Krajnovic, Sinisa, and Lars Davidson. "Development of large-eddy simulation for vehicle aerodynamics." In *ASME 2002 International mechanical engineering congress and exposition*, pp. 165-172. American Society of Mechanical Engineers, 2002.
[13] Spohn, A., and P. Gilliéron. "Flow separations generated by a simplified geometry of an automotive vehicle." In *IUTAM Symposium: unsteady separated flows*, pp. 8-12. 2002.
[14] M.Kanagaraj, Dr.S.Periyasamy. "Drag reduction using vortex generator on a passenger vehicle." *International Journal of Innovative Research in Science, Engineering and Technology* 6, no.7 (2017):83-88.
[15] G.Sivaraj, D.Lakshmanan, R.Veeramanikandan. "The computational analysis of sedan car with vortex generator." *International Journal of Advance Research in Science and Engineering* 4, no. 1 (2015): 1531-1537.
[16] FLUENT Europe, "FLUENT 6: User's Guide.", FLUENT Incorporated., 2002.
[17] Roache, Patrick J., Kirti N. Ghia, and Frank M. White. "Editorial policy statement on the control of numerical accuracy." *Journal of Fluids Engineering* 108, no. 1 (1986): 2-2.